

Turbulent exchange of heat, water vapor, and momentum over a Tibetan prairie by eddy covariance and flux variance measurements

Taejin Choi,¹ Jinkyu Hong,¹ Joon Kim,¹ Heechoon Lee,¹ Jun Asanuma,² Hirohiko Ishikawa,³ Osamu Tsukamoto,⁴ Gao Zhiqiu,⁵ Yaoming Ma,⁶ Kenichi Ueno,⁶ Jiemin Wang,⁷ Toshio Koike,⁸ and Tetsuo Yasunari⁹

Received 12 March 2004; revised 28 July 2004; accepted 1 September 2004; published 6 November 2004.

[1] Land-atmosphere interactions on the Tibetan Plateau are important because of their influence on energy and water cycles on both regional and global scales. Flux variance and eddy covariance methods were used to measure turbulent fluxes of heat, water vapor, and momentum over a Tibetan shortgrass prairie during the Global Energy and Water Cycle Experiment (GEWEX) Asian Monsoon Experiment (GAME) in 1998. Under unstable conditions during the monsoon period (July–September), the observed standard deviations of temperature and specific humidity (normalized by appropriate scaling parameters) followed the Monin-Obukhov theory. The similarity constants for heat C_T and water vapor C_q in their dimensionless functions of stability under a free convection limit were both 1.1, unlike the differences (i.e., $C_T \leq C_q$) reported in other studies. While the transfer efficiency of heat and water vapor exchange generally agreed with the prediction from the Monin-Obukhov theory, momentum exchange was less efficient than predicted. In comparison with the eddy covariance data, the flux variance method (with $C_T = C_q = 1.1$) underestimated both heat and water vapor fluxes by <5%. When the eddy covariance data were absent, the flux variance method was used for gap filling the seasonal flux database. To estimate latent heat flux during the premonsoon period in June, C_T/C_q was approximated as r_{Tq} (where r_{Tq} is a correlation coefficient for the fluctuations of temperature and water vapor) because of the sensitivity of C_q to changes in soil moisture conditions. The dramatic changes in the Bowen ratio from 9.0 to 0.4 indicate the shift of energy sources for atmospheric heating over the plateau, which, in turn, resulted in the shift of turbulent exchange mechanisms for heat and water vapor. **INDEX TERMS:** 1878 Hydrology: Water/energy interactions; 0315 Atmospheric Composition and Structure: Biosphere/atmosphere interactions; 3307 Meteorology and Atmospheric Dynamics: Boundary layer processes; 3379 Meteorology and Atmospheric Dynamics: Turbulence; **KEYWORDS:** Tibetan Plateau, eddy covariance, flux variance, Monin-Obukhov theory

Citation: Choi, T., et al. (2004), Turbulent exchange of heat, water vapor, and momentum over a Tibetan prairie by eddy covariance and flux variance measurements, *J. Geophys. Res.*, 109, D21106, doi:10.1029/2004JD004767.

1. Introduction

[2] The Tibetan Plateau is characterized by high elevation (>4000 m) and vast area ($\sim 10^\circ$ in latitude and $\sim 25^\circ$ in

longitude). The plateau has been the subject of climate research for several decades because of its topographic characteristics and its influence on energy and water cycles on both regional (e.g., Asian monsoon) and global (e.g., El Niño) scales [e.g., Flohn, 1957; Yeh et al., 1957; Liu et al., 2003]. The onset of the Asian summer monsoon coincides with the reversal of the meridional temperature gradient in the upper troposphere south of the Tibetan Plateau, resulting from the large temperature increases in May to June over Eurasia and centered on the plateau [Li and Yanai, 1996].

[3] Much effort has been made to evaluate the strength and distribution of atmospheric heat and moisture sources over the plateau and its vicinity. Researchers have found that: (1) the plateau is the major energy source by providing sensible heat flux to the atmosphere before the onset of monsoon [e.g., Li and Yanai, 1996]; (2) during the rainy season, the latent heat released to the atmosphere is the dominant heat source over the eastern plateau, whereas

¹Department of Atmospheric Sciences, Yonsei University, Seoul, Republic of Korea.

²Department of Geosciences, Tsukuba University, Tsukuba, Japan.

³Disaster Prevention Research Institute, Kyoto University, Kyoto, Japan.

⁴Faculty of Science, Okayama University, Okayama, Japan.

⁵Chinese Administration for Meteorological Sciences, Beijing, China.

⁶School of Environment, University of Shiga Prefecture, Shiga, Japan.

⁷Cold and Arid Regions Environmental and Engineering Research Institute, Chinese Academy of Sciences, Lanzhou, China.

⁸Department of Civil Engineering, University of Tokyo, Tokyo, Japan.

⁹Hydrospheric Atmospheric Research Center, Nagoya University, Nagoya, Japan.

sensible heat flux is comparable to latent heat flux over the western plateau [e.g., *Chen et al.*, 1985]; (3) local recycling through evaporation is important in the water budget over the western plateau, whereas water vapor transport from outside is significant over the eastern plateau [e.g., *Luo and Yanai*, 1983]; and (4) there is a consensus on the distribution of heat/moisture sources and the heating mechanism over the plateau, but the magnitudes are conflicting. For instance, *Yeh and Gao* [1979] obtained a vertically integrated mean heat source of 138 Wm^{-2} over the western plateau in June, whereas *Chen et al.* [1985] estimated it as 37 Wm^{-2} . This large discrepancy was caused by the different drag coefficients used in the bulk method, resulting in different sensible heat fluxes by a factor of 2–3. *Li et al.* [2001] reported a wide range of drag coefficients (i.e., 2.5×10^{-3} to 12×10^{-3}) over the plateau despite the use of the same data. Latent heat flux can be estimated as a residual of the surface energy budget. However, this approach is prone to error because significant lacks (10–40%) in the energy budget closure on the plateau have been reported [e.g., *Kim et al.*, 2001; *Bian et al.*, 2002].

[4] The paucity of direct flux measurements has hindered us from better understanding the role of the Tibetan Plateau in the cyclic processes of energy and water and their potential alteration associated with global change. Consequently, the Global Energy and Water Cycle Experiment (GEWEX) Asian Monsoon Experiment (GAME) was organized and intensive field measurement campaigns were executed on the plateau in 1998 [e.g., *Koike et al.*, 1999]. Since 2002, further long-term flux measurements have been attempted through the Coordinated Enhanced Observing Period (CEOP, <http://monsoon.t.u-tokyo.ac.jp/ceop/>). In these efforts, the eddy covariance method has been used to quantify the seasonal changes in surface energy partitioning.

[5] The objective of this paper is to investigate turbulent exchange characteristics over a Tibetan prairie in terms of flux variance relations, and to document the seasonal changes in surface energy partitioning. Both eddy covariance and flux variance methods were employed to measure the turbulent fluxes from late May to September in 1998. We have used flux variance when the eddy covariance method was not possible because of breakage of the sonic anemometer under the extreme environmental conditions on the plateau. The validity of the use of flux variance is thus tested against direct measurement by eddy covariance. Basic characteristics of turbulence statistics are analyzed to understand the mechanisms controlling the surface exchange of energy and water. The flux data obtained from the two methods are combined to examine the seasonal variation of energy partitioning associated with the monsoon. The gap-filled flux data have been documented in a public domain database for further use in validating and calibrating of various land surface models.

2. Materials and Method

2.1. Theoretical Considerations

2.1.1. Eddy Covariance Method

[6] Vertical flux F of any scalar is based on the conservation equation. If the site is homogeneous and flat, and assuming stationarity and no sink/source for the scalar, then F can be obtained from the covariance between the

fluctuations of vertical wind velocity w and a mixing ratio of scalar χ as below [e.g., *Swinbank*, 1951].

$$F = \rho_a \overline{w'\chi'}, \quad (1)$$

where ρ_a is the air density ($\sim 0.71 \text{ kg m}^{-3}$ at the study site), and the overbar and primes denote time averaging and fluctuations from the mean, respectively.

2.1.2. Flux Variance Method

[7] On the basis of the Monin-Obukhov similarity theory, standard deviations of any quantity, x such as w , longitudinal wind speed u , temperature T and specific humidity q normalized by scaling parameters become universal functions of z/L as [e.g., *Tillman*, 1972]:

$$\sigma_x/x_* = \phi_x(z/L) = C_{x1}(1 - C_{x2}z/L)^{\pm 1/3}, \quad (2)$$

where σ_x is the standard deviation of x , x_* is the scaling parameter ($\equiv \overline{w'x'_0}/u_*$, where $\overline{w'x'_0}$ is the flux at the surface and u_* is the friction velocity), ϕ_x is the normalized function, z is the measurement height, L is the Obukhov length, and C_{x1} and C_{x2} are empirical constants. Positive (negative) sign corresponds to wind components (scalars). As $-z/L$ approaches infinity (i.e., local free convection), equation (2) can be simplified as [e.g., *Wjngaard et al.*, 1971]:

$$\sigma_x/x_* = \phi_x(z/L) = C_x(-z/L)^{\pm 1/3}, \quad (3)$$

where $C_x (= C_{x1}C_{x2}^{\pm 1/3})$ is a similarity constant. Taking T as x and rearranging equation (3), sensible heat flux H is expressed as [e.g., *Katul et al.*, 1995].

$$H = c_p \rho_a \left(\frac{\sigma_T}{C_T} \right)^{3/2} \left(\frac{kgz}{T} \right)^{1/2}, \quad (4)$$

where c_p is the specific heat capacity of dry air at constant pressure ($= 1005 \text{ Jkg}^{-1} \text{ K}^{-1}$), C_T is a similarity constant for heat, k is the von Kármán constant ($= 0.4$), and g is the acceleration due to gravity.

[8] Water vapor flux is better estimated using a site-specific similarity constant for water vapor C_q determined under free convection limit than using values in the literature [*Asanuma and Brutsaert*, 1999];

$$\lambda E = \lambda \rho_a \frac{C_T}{C_q} \frac{\sigma_q}{\sigma_T} \overline{w'T'} = \lambda \rho_a \frac{r_{wq}}{r_{wT}} \frac{\sigma_q}{\sigma_T} \overline{w'T'}, \quad (5)$$

where r_{wT} and r_{wq} are the correlation coefficients for w' and T' , and w' and q' , respectively.

[9] The value of C_T seems universal and independent on surface conditions, unlike that of C_q [e.g., *Weaver*, 1990; *De Bruin et al.*, 1993; *Andreas et al.*, 1998]. The latter increases pronouncedly as r_{Tq} decreases [*Asanuma and Brutsaert*, 1999]. The surface moisture condition at our study site changed dramatically as the summer monsoon progressed. We therefore assume that C_T does not change through the season, whereas C_q changes with soil water availability.

[10] The term, r_{wT}/r_{wq} in equation (5) could be approximated by r_{Tq} when $r_{wT}/r_{wq} < 1$ (or $1/r_{Tq}$ when $r_{wT}/r_{wq} > 1$)

[Bink and Meesters, 1997; Katul and Hsieh, 1997]. Then, we can rewrite equation (5) as

$$\lambda E = \lambda \rho_a \frac{1}{r_{Tq}} \frac{\sigma_q \overline{w'T'}}{\sigma_T} \quad \text{if } r_{wT} < r_{wq} \quad (6a)$$

$$\lambda E = \lambda \rho_a r_{Tq} \frac{\sigma_q \overline{w'T'}}{\sigma_T} \quad \text{if } r_{wT} > r_{wq}. \quad (6b)$$

Figure 1a shows the relationship between r_{Tq} (or $1/r_{Tq}$) and r_{wT}/r_{wq} at the study site (BJ site), indicating that equations (6a) and (6b) hold. When quadrant analysis is applied to remove the likely effect of entrainment from the ABL top on r_{Tq} , better relationship is obtained (Figure 1b).

2.1.3. Correlation Coefficients

[11] The vertical transfer efficiencies for heat and water vapor can be evaluated by their correlation coefficients, r_{wT} and r_{wq} , respectively. The ratio of r_{wT} to r_{wq} represents the relative transfer efficiency. On the basis of the Monin-Obukhov similarity theory, r_{wx} can be predicted using the corresponding integral turbulence characteristics (ITC) [e.g., De Bruin *et al.*, 1993]:

$$r_{wx} = \frac{\overline{w'c'}}{\sigma_w \sigma_x} = \left(1 - C_{x2} \frac{z}{L}\right)^{\pm 1/3} / C_{w1} C_{x1} \left(1 - C_{w2} \frac{z}{L}\right)^{1/3}. \quad (7)$$

If x is scalar, the numerator is $[1 - C_{x2}(z/L)]^{1/3}$. Otherwise, $[1 - C_{x2}(z/L)]^{-1/3}$ is used.

2.1.4. Drag Coefficients

[12] Drag coefficients C_D at the reference height (i.e., 10 m) and under neutral stability (C_{DN10}), can be evaluated through the relation [e.g., Andreas *et al.*, 1998],

$$C_{DN10} = \frac{k^2}{[\ln(10/z_0)]^2}, \quad (8)$$

where z_0 is the roughness length for momentum.

2.2. Site and Measurements

2.2.1. Study Site

[13] The field experiment was conducted at a shortgrass prairie (BJ site) near Naqu (92.04°E, 31.29°N, 4580 m above m.s.l.), Tibet in China. Soil was predominantly sandy silt loam at the site, which was homogeneous and flat with a fetch of >1 km for the prevailing wind directions. The flux measurement was made from late May to mid-September in 1998. The rainy season started in late June. During the premonsoon period the surface was dry and sparsely covered with short grasses. With the onset of the monsoon, the volumetric soil water content remained >15% and the average grass height was about 0.05 m with grazing.

2.2.2. Flux Measurement

[14] The eddy covariance measurement system consisted of a three-dimensional sonic anemometer (CSAT3, Campbell Scientific, Inc.), a krypton hygrometer (KH20, Campbell Scientific, Inc.), and a fine-wire thermocouple. Measurements were taken 2.85 m above the ground, and the separation between the sonic anemometer and the hygrometer was 0.15 m. The prevailing wind direction was from 135° to 225°. The sampling rate was 20 Hz and the raw data were saved on

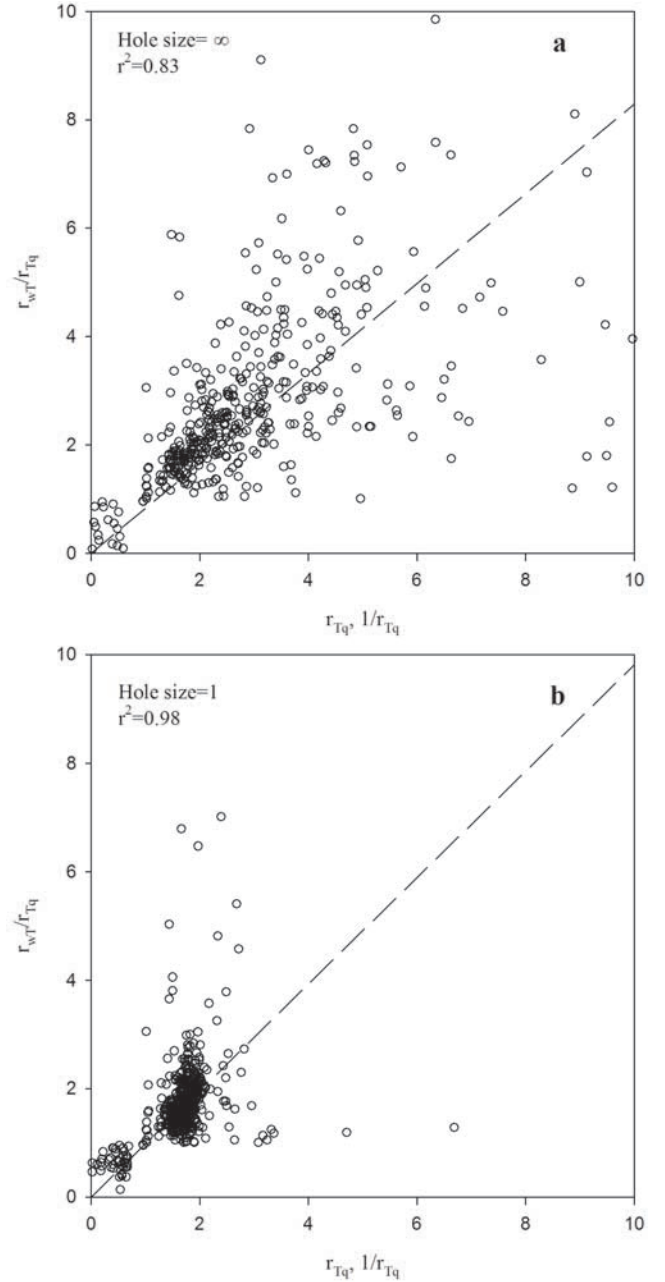


Figure 1. Relationship between r_{Tq} (or $1/r_{Tq}$) and r_{wT}/r_{wq} at the study site from July to September in 1998: (a) with the whole data set and (b) with reduced data set of the quadrant analysis.

a laptop computer connected to a data logger (CR9000, Campbell Scientific, Inc.) for postprocessing. Half-hourly averaged turbulence statistics were calculated and recorded on the data logger.

[15] Because of long and rough transportation to the experimental site, the sonic anemometer was broken and was not replaced until 14 July. During this period standard deviations of temperature and humidity were measured with fine wire thermocouples and a krypton hygrometer, respectively. Because of a wide range of humidity, the path length of krypton hygrometer was adjusted, and the instrument was calibrated again in a low-pressure chamber after the experiment.

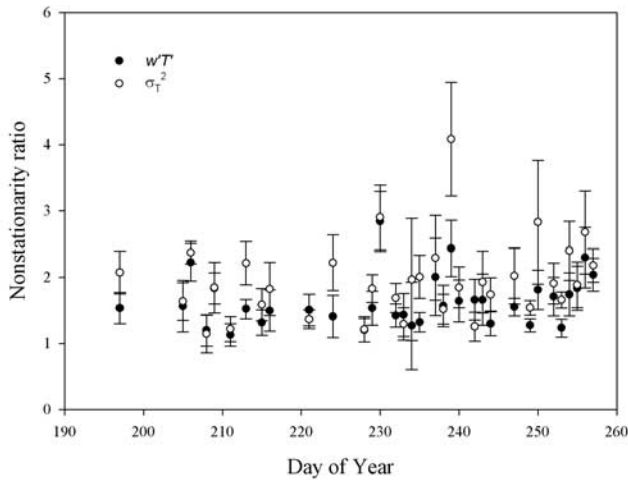


Figure 2. Variations of daytime-averaged nonstationarity ratio NR for $w'T'$ and variance of temperature σ_T^2 during the monsoon period. Error bars indicate standard error of mean.

[16] Other supporting micrometeorological measurements made at the site included radiation components, soil heat flux, soil temperature, soil water content, air temperature and humidity, wind speed, and direction. All these slow-response signals were sampled every 30 s. Average values for 30-min periods were stored on the same data logger. Electrical power was not available, and thus all the instruments and the data-logging system were operated through 12 VDC batteries that were recharged by solar panels [Kim *et al.*, 2001].

2.2.3. Flux Corrections

[17] The effect of coordinate rotation on fluxes was less than 1%. To further evaluate the contribution of low-frequency eddies [e.g., Finnigan *et al.*, 2003], half-hourly averaged fluxes were compared against 2-hour averages and the agreement was within 1%. Following Moore [1986], fluxes were adjusted for the effects of path length averaging and sensor separation, resulting in 5% increase in latent heat flux. Further correction for the density variation was applied to latent heat flux [Webb *et al.*, 1980].

2.2.4. Stationarity Test

[18] To satisfy the stationarity assumption, the statistical properties of the measured time series should not change with time. To evaluate the degree to which turbulent statistics may violate this assumption, the nonstationarity ratio (NR) is defined as [Mahrt, 1998]

$$\text{NR} \equiv \sigma_{btw}/\text{RE}, \quad (9)$$

where σ_{btw} is the between-record standard deviation of statistics (for this analysis, half-hourly raw data were divided into four records), and RE ($=\sigma_{wi}/\sqrt{J}$) is the random error estimate, where σ_{wi} is the averaged within-record standard deviation over all of the records, and J is the number of subrecord segments (six segments per record were used for this study). While RE has the effect of random variability on turbulence statistics only, σ_{btw} may be affected by both nonstationarity and random variability. Ideally, NR = 1 if the turbulence statistics are stationary. In practice, data are

considered nonstationary when $\text{NR} \gg 2$ [Mahrt, 1998]. The NR values for daytime averaged $w'T'$ and σ_T^2 in Figure 2 show that the stationarity requirement is generally met.

3. Results and Discussion

3.1. Turbulence Characteristics

[19] The measured σ_w/u_* is plotted with $-z/L$ in Figure 3a. A normalized function of σ_w/u_* ($=C_{w1}(1 + C_{w2}|z/L|)^{1/3}$) was determined, resulting in $C_{w1} = 1.12$ and $C_{w2} = 2.8$. Also presented is the formulation of Kaimal and Finnigan [1994] (i.e., $\sigma_w/u_* = 1.25(1 + 3|z/L|)^{1/3}$), which predicts consistently greater σ_w/u_* . Similar results were obtained from data collected 20 m above ground using taller towers: one at the BJ site in 2002 and the other at Anni site in 2003 [Hong *et al.*, 2004]. The σ_w/u_* value of ~ 1.12 under near-neutral conditions is within the range reported in the literature [i.e., Kaimal and Finnigan, 1994; Pahlow *et al.*, 2001]. Pattey *et al.* [2002] show that σ_w/u_* can vary depending on the types of sonic anemometers, particularly with one with longer path length due to loss of covariance between u and w .

[20] The measured σ_u/u_* is plotted with $-z/L$ in Figure 3b. Its normalized function is $3.13(1 + 8|z/L|)^{1/3}$. In comparison with σ_w/u_* , more scatters are evident with σ_u/u_* . The latter may not totally follow the Monin-Obukhov theory and be better scaled with boundary layer depth h_i [Panofsky and Dutton, 1984; Van Den Hurk and De Bruin, 1995]. However, σ_u/u_* in Figure 3b did not scale with h_i/L , where h_i was given as constant. The normalized function ($\sigma_u/u_* = 2.2(1 + 3|z/L|)^{1/3}$) of De Bruin *et al.* [1993] underestimates the observed σ_u/u_* .

[21] The measured r_{uw} is presented in Figure 4 with the correlation function (equation (7) with $C_{u1} = 3.13$, $C_{u2} = 8$, $C_{w1} = 1.12$, and $C_{w2} = 2.8$). The r_{uw} decreases in magnitude with increasing stability because of the dominant role of buoyancy production over shear production. The measured r_{uw} appears to follow the expected pattern as a function of $-z/L$ but with magnitudes smaller than those predicted. The normalized function of De Bruin *et al.* [1993] underestimates the r_{uw} , indicating a lower efficiency of momentum exchange over the Tibetan Plateau than over terrains at low altitudes.

[22] To investigate whether the cause of such smaller r_{uw} observed with the Campbell sonic anemometer could be instrumental, the data obtained during the intercomparison study with a different sonic anemometer (DAT-600, Kaijo Denki) were also examined. The result, however, was similar, indicating no instrumental bias [see also Hong *et al.*, 2004]. Högstrom [2002] and McNaughton and Brunet [2002] point out a role of inactive eddies that decreases r_{uw} through the enhanced σ_u . Indeed, on the basis of spectrum analyses of u and v under near-neutral conditions, Hong *et al.* [2004] show the evidence of such inactive eddies (i.e., large spectral density at low-frequency range) at the BJ site.

[23] Figure 5 shows σ_T/T_* and σ_q/q_* under unstable to near-neutral conditions. Except for the scatters under near-neutral conditions, the measured σ_T/T_* follows well the Monin-Obukhov theory under unstable conditions. The data in Figure 5a fitted to a normalized function (i.e., $\sigma_T/T_* = C_{T1}(1 + C_{T2}|z/L|)^{-1/3}$) resulted in $C_{T1} = 3.7$ and $C_{T2} = 34.5$. (To minimize the effect of scattered data, the data were

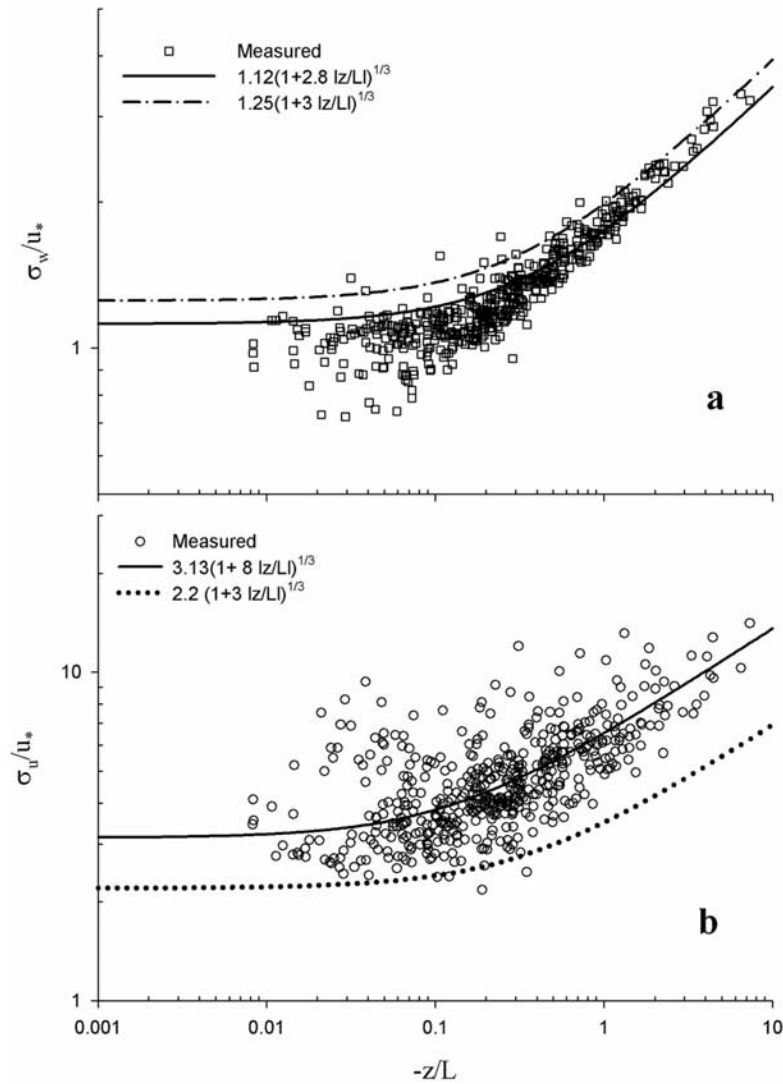


Figure 3. Integral turbulence characteristics of (a) vertical and (b) streamwise wind component with $-z/L$ during the monsoon period. Solid lines are the normalized functions from this study, the dash-dotted line is that by *Kaimal and Finnigan* [1994], and the dotted line is that by *De Bruin et al.* [1993].

selected when $r_{Tq} > 0.9$.) For comparison, the normalized functions for heat of *Kaimal and Finnigan* [1994] and *Andreas et al.* [1998] are also presented in Figure 5. The normalized function for σ_T/T_* in our study is almost identical to that of *Andreas et al.* [1998] over a terrain with patchy vegetation with height of <0.6 m. However, the magnitudes of σ_T/T_* in our study are greater than those from the Kansas data [*Kaimal and Finnigan*, 1994].

[24] Surprisingly, the behavior of σ_q/q_* is markedly similar to that of heat (Figure 5b). Unlike σ_T/T_* , the normalized function for σ_q/q_* of *Andreas et al.* [1998] overestimates σ_q/q_* . A normalized function for σ_q/q_* is not given by *Kaimal and Finnigan* [1994] but is suggested to have a functional form similar to that for σ_T/T_* (also shown in Figure 5b for comparison).

[25] Figure 6 shows the behavior of σ_T/T_* and σ_q/q_* within the free convection limit ($-z/L > 0.2$). The similarity constant in a simplified function (i.e., C_x in equation (3)) is 1.1 for both C_T and C_q . In the literature, C_T ranges from 0.91

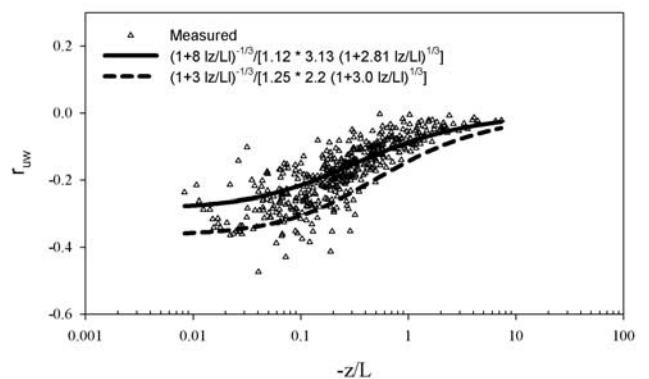


Figure 4. Variation of correlation coefficients for w and u during the monsoon period. The solid line is predicted by the corresponding ITCs in this study, and the dashed line is provided by *De Bruin et al.* [1993].

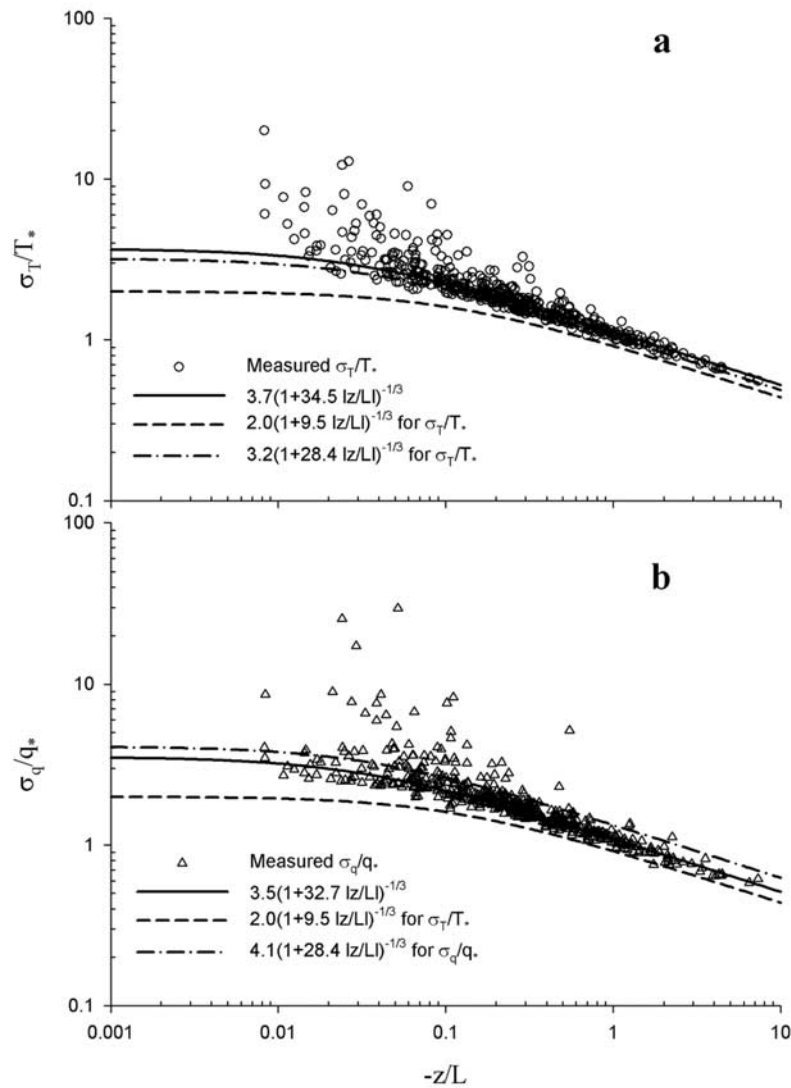


Figure 5. Integral turbulence characteristics of (a) heat and (b) water vapor near neutral and under unstable stability during the monsoon period. Solid lines are the fitted normalized functions for σ_T/T_* and σ_q/q_* from this study, dashed lines are those by *Kaimal and Finnigan* [1994], and dash-dotted lines are those by *Andreas et al.* [1998].

to 1.12 whereas C_q is greater, with a range of 1.1–1.5 [e.g., *Asanuma and Brutsaert*, 1999; *Katul and Hsieh*, 1999]. On the basis of the analysis of covariance budget equations for $\overline{w'T'}$ and $\overline{w'q'}$, *Katul and Hsieh* [1999] showed that $C_T < C_q$, suggesting a dissimilarity between heat and water vapor.

[26] In Figure 7, the transfer efficiency of heat to water vapor (i.e., r_{wT}/r_{wq}) is plotted against $-z/L$. Except the scatters toward near-neutral conditions, the data converge to unity under unstable conditions, suggesting a similarity of source/sink between heat and water vapor near the ground surface.

[27] The measured r_{wT} and r_{wq} are shown in Figure 8 with equation (7) (with the predetermined constants: $C_{x1} = 3.7$, $C_{x2} = 34.5$, $C_{w1} = 1.12$, and $C_{w2} = 2.8$). Both r_{wT} and r_{wq} increase as the stability becomes more unstable. For comparison, the formulation of *De Bruin et al.* [1993] is also included. Both r_{wT} and r_{wq} show that each scalar follows the Monin-Obukhov theory with similar transfer efficiency.

[28] Figure 9 shows the transfer efficiencies of heat and water vapor as compared to momentum. Heat and water vapor are transferred more efficiently than momentum over a range of different stabilities. While the momentum exchange is systematically less efficient, heat and water vapor exchange shows a similar efficiency in magnitude, following the Monin-Obukhov theory.

3.2. Drag Coefficients

[29] First, z_0 is estimated on the basis of logarithmic wind profiles under neutral conditions ($-0.05 < z/L < 0.05$). By substituting the estimated $z_0 (= 0.009 \pm 0.009 \text{ m})$ in equation (8), C_{DN} is estimated to be $3.1 (\pm 0.7) \times 10^{-3}$. On the basis of wind profile measurements at the same site, *Gao et al.* [2000] reported z_0 of 0.0113 m and C_{DN} of 3.5×10^{-3} . *Li et al.* [2001] estimated the drag coefficients at four stations on the plateau using wind profile measurements over 6 years and obtained $4.4\text{--}4.7 \times 10^{-3}$. *Bian et al.*

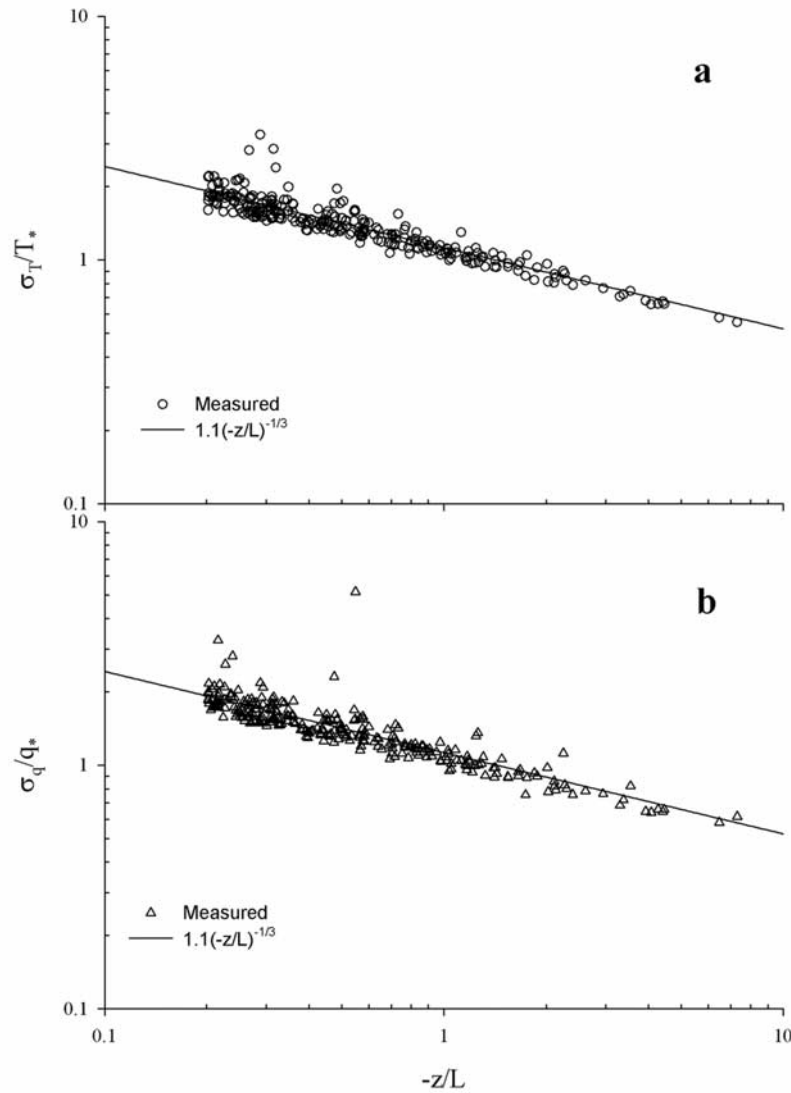


Figure 6. Integral turbulence characteristics of (a) T and (b) q under free convection ($-z/L > 0.2$) during the monsoon period. Solid lines are the regression lines fitted to the measurements from this study.

[2002] obtained C_{DN} of 5.5×10^{-3} through turbulence measurements at Qando site with sparse weeds of 0.35 m height in the southeastern Tibetan Plateau. Overall, these recent estimates of drag coefficients are only half of those ($6 \sim 8 \times 10^{-3}$) reported by earlier studies [e.g., Yeh and Gao, 1979].

3.3. Flux Comparison Between Eddy Covariance and Flux Variance Methods

[30] Sensible heat H_{VAR} and latent heat fluxes λE_{VAR} from the flux variance method were calculated using equations (4) and (5), respectively (with $C_T = C_q = 1.1$) and compared against the available eddy covariance fluxes (H_{EC} and λE_{EC}) for the same period. The fluxes from the two methods agree within 5% ($SEE = 12 \text{ Wm}^{-2}$ and $r^2 = 0.88$ for H ; $SEE = 37 \text{ Wm}^{-2}$ and $r^2 = 0.78$ for λE).

[31] Because of changes in C_q with varying soil water conditions, λE_{VAR} was also computed with equations (6a) and (6b) using r_{Tq} and $1/r_{Tq}$. Again, the flux comparison between the two methods is similar to that with a constant

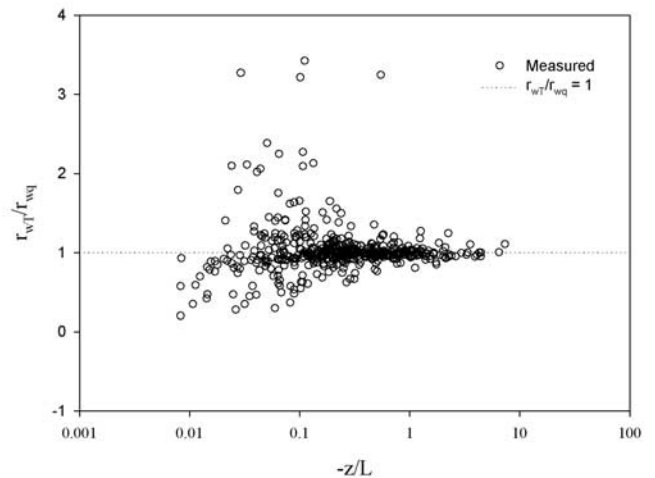


Figure 7. Variation of r_{wT}/r_{wq} with $-z/L$ under near-neutral and unstable conditions during the monsoon period. The dotted line shows $r_{wT}/r_{wq} = 1$.

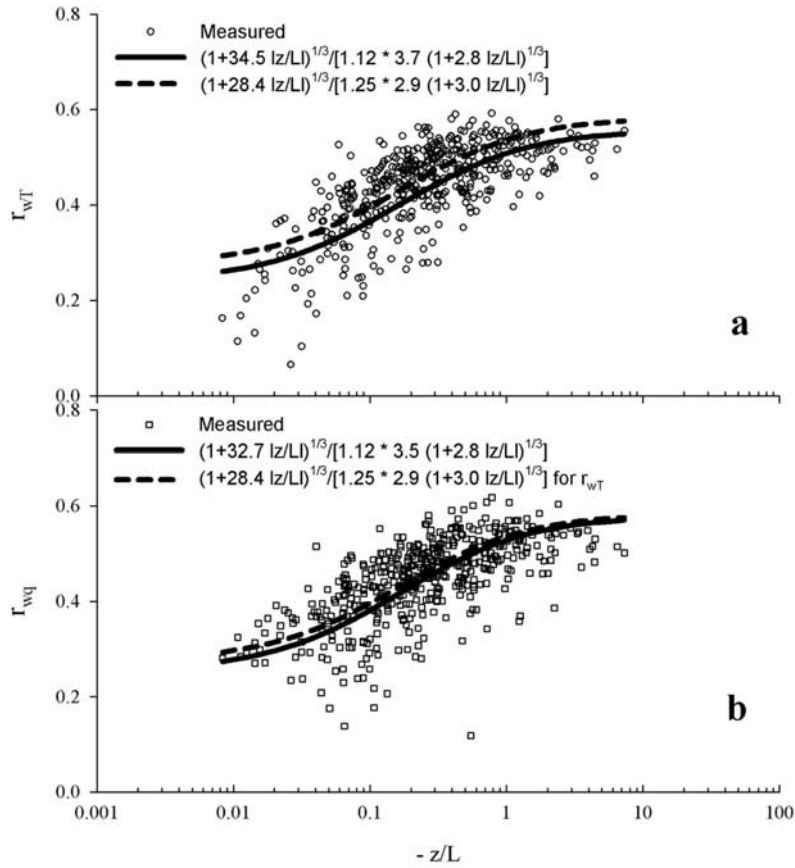


Figure 8. Variation of correlation coefficients for (a) w and T and (b) w and q during the monsoon period. Solid lines are predicted by the corresponding ITCs in this study, and dashed lines for each correlation are provided by *De Bruin et al.* [1993].

C_q , except for larger values of $SEE(=74 \text{ Wm}^{-2})$ and lower $r^2(=0.34)$ (Figure 10b). This is mainly due to small r_{Tq} , resulting in $1/r_{Tq}$ of much larger than 1.1. It is encouraging, however, that λE_{VAR} using r_{Tq} is comparable to the measured λE_{EC} . This result provides good grounds for applying the flux variance method when eddy covariance measurement is not available.

3.4. Seasonal Variations of Energy Partitioning and Turbulent Exchange Mechanism

[32] As the summer monsoon advanced, there were significant changes in meteorological conditions, surface energy partitioning and turbulent exchange characteristics.

3.4.1. Precipitation and Land Cover

[33] Figure 11 shows the seasonal variations of precipitation and soil water content (0.1 m layer). Frequency and magnitude of precipitation increased particularly in late June, resulting in a rapid increase in soil water content. From the green-up stage in late June to peak growth in July–August, the approximate leaf area index (LAI) increased up to 0.45, with a mean canopy height of 0.05 m [Gao et al., 2004]. Following the change in vegetation cover, color and soil water conditions at the site, the radiation balance changed dramatically.

3.4.2. Radiation Balance

[34] Figure 12 shows the diurnal variation of radiation components on two fairly clear days (12 June and 9 August

1998). Prior to monsoon (12 June), the daytime outgoing longwave radiation R_{lup} and incoming longwave radiation R_{ldn} reached up to 600 Wm^{-2} and 300 Wm^{-2} , respectively. The R_{lup} is significantly larger than those at low altitudes in

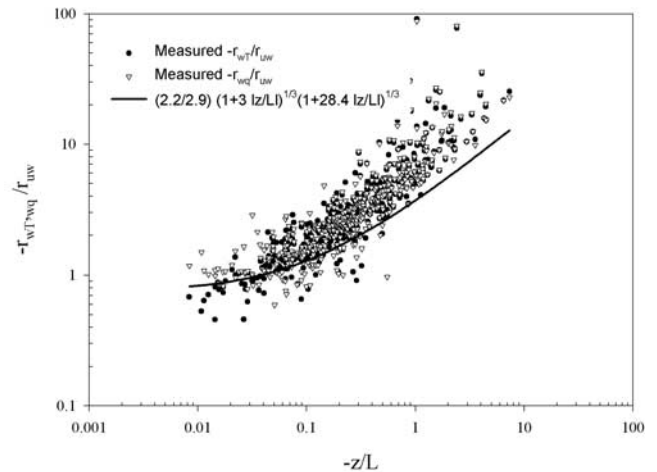


Figure 9. Transfer efficiencies of heat and water vapor to momentum under near-neutral and unstable conditions during the monsoon period. The solid line is the formulation from *De Bruin et al.* [1993].

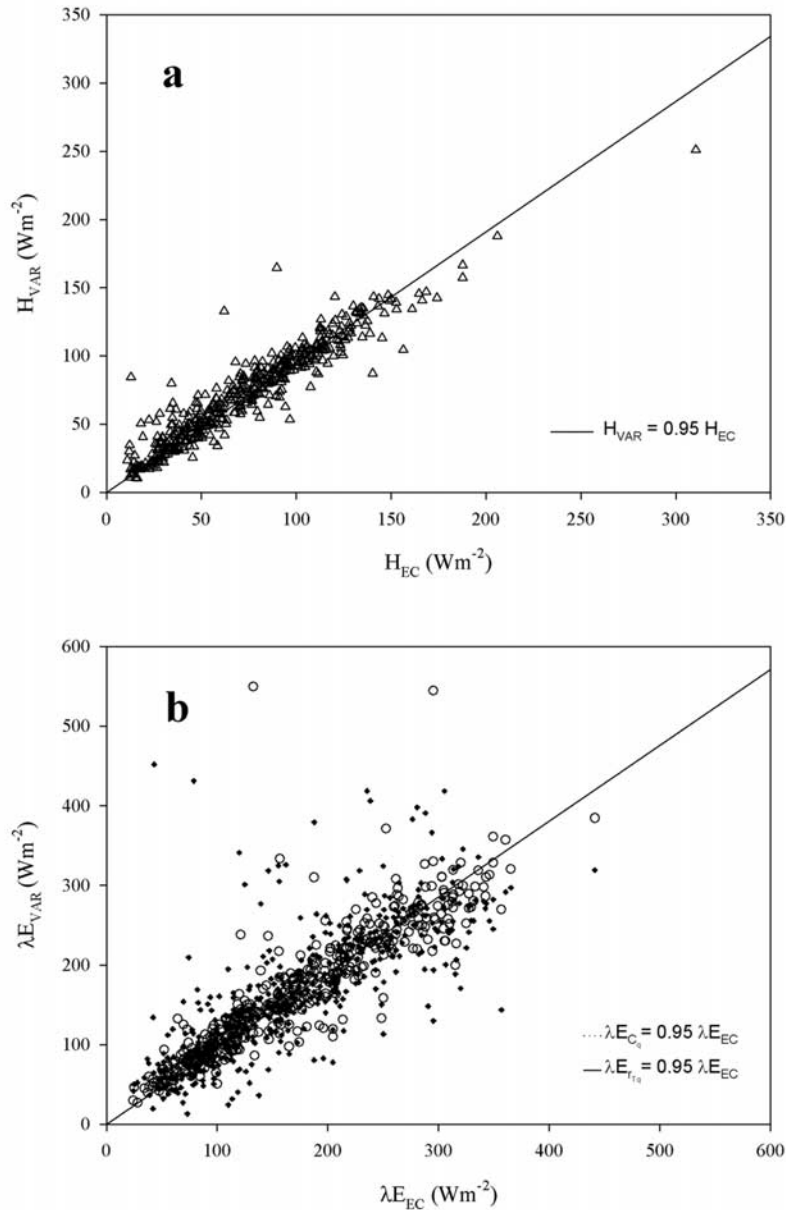


Figure 10. Comparison of measured fluxes of (a) sensible heat and (b) latent heat with estimated ones. The open circles represent latent heat flux λE_{C_q} from the flux variance method using C_q of 1.1, and the pluses represent latent heat flux $\lambda E_{r_{Tq}}$ from flux variance method using r_{Tq} (or $1/r_{Tq}$).

similar latitudes. *Smith and Shi* [1992] also reported large values of R_{lup} over the Tibetan Plateau. During the monsoon (9 August), R_{lup} decreased by 30% but R_{ldn} increased by 20%, resulting in 60% increase in net longwave radiation. While downward shortwave radiation R_{sdn} remained almost the same, the albedo ($=R_{sup}/R_{sdn}$) decreased by 30% from premonsoon (0.2) to monsoon (0.15). Consequently, the net radiation (R_n) increased by 20%. During midday, about 25% of R_n was dissipated into soil heat flux.

3.4.3. Surface Energy Partitioning

[35] Figure 13 shows the seasonal variation of the energy partitioning in terms of the Bowen ratio ($\beta = H/\lambda E$). With the onset of the summer monsoon, β decreased rapidly from 9 in early June to 0.4 in July and remained low until mid-September. Then, β began to increase with the withdrawal

of the monsoon. Prior to the monsoon, sensible heat flux from the surface was the major source of heating over the plateau, whereas the latent heat released by condensation became the primary source with the onset of the monsoon.

3.4.4. Shift in Turbulent Exchange Mechanism

[36] The seasonal variation of daytime averaged r_{Tq} increases from near zero during the premonsoon to 0.8 during the monsoon period (Figure 14). Such a change in r_{Tq} implies a shift in the similarity between heat and water vapor with the seasonal march of summer monsoon. Changes in skewness of $T(Sk_T)$, $q(Sk_q)$ and $w(Sk_w)$ provide further insights. Normally, positive skewness values are expected because of narrow, warm and moist updrafts, compared to wider, cool and dry downdrafts [Mahrt, 1991]. Throughout the season, Sk_T and Sk_w are consistently

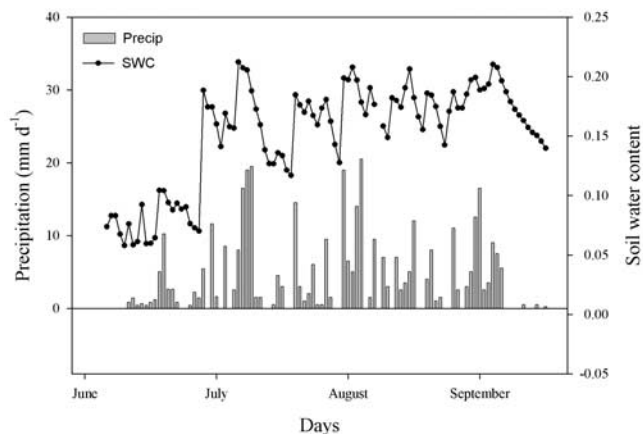


Figure 11. Seasonal variations of precipitation and soil water content (SWC).

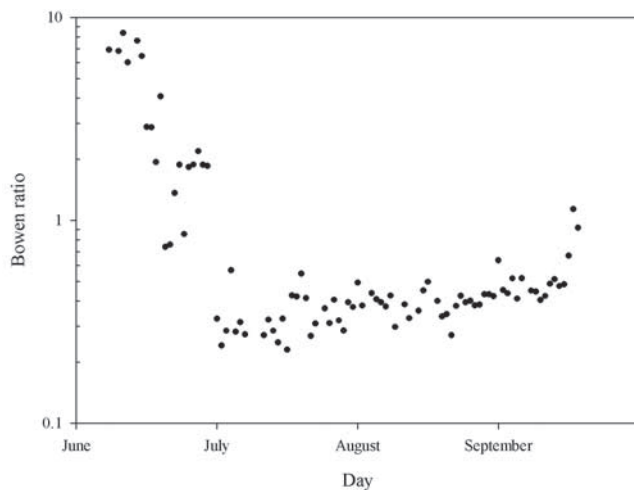


Figure 13. Seasonal variation of the Bowen ratio.

positive ($0.2 \sim 1.5$). However, as β rapidly decreases with enhanced λE , Sk_q shifts from negative to near-zero values in June to positive values comparable to Sk_T during the monsoon period. *Mahrt* [1991] reported that r_{Tq} and Sk_q (measured at 100–150 m above ground) increased with

decreasing boundary layer height because of strong surface evaporation. During our study, h_i over Amdo site (~ 100 km north of BJ site) also decreased from ~ 2.5 km during premonsoon to about 1 km during monsoon period in 1998 (<http://monsoon.t.u-tokyo.ac.jp/tibet/data/iop/pbltower/>). As

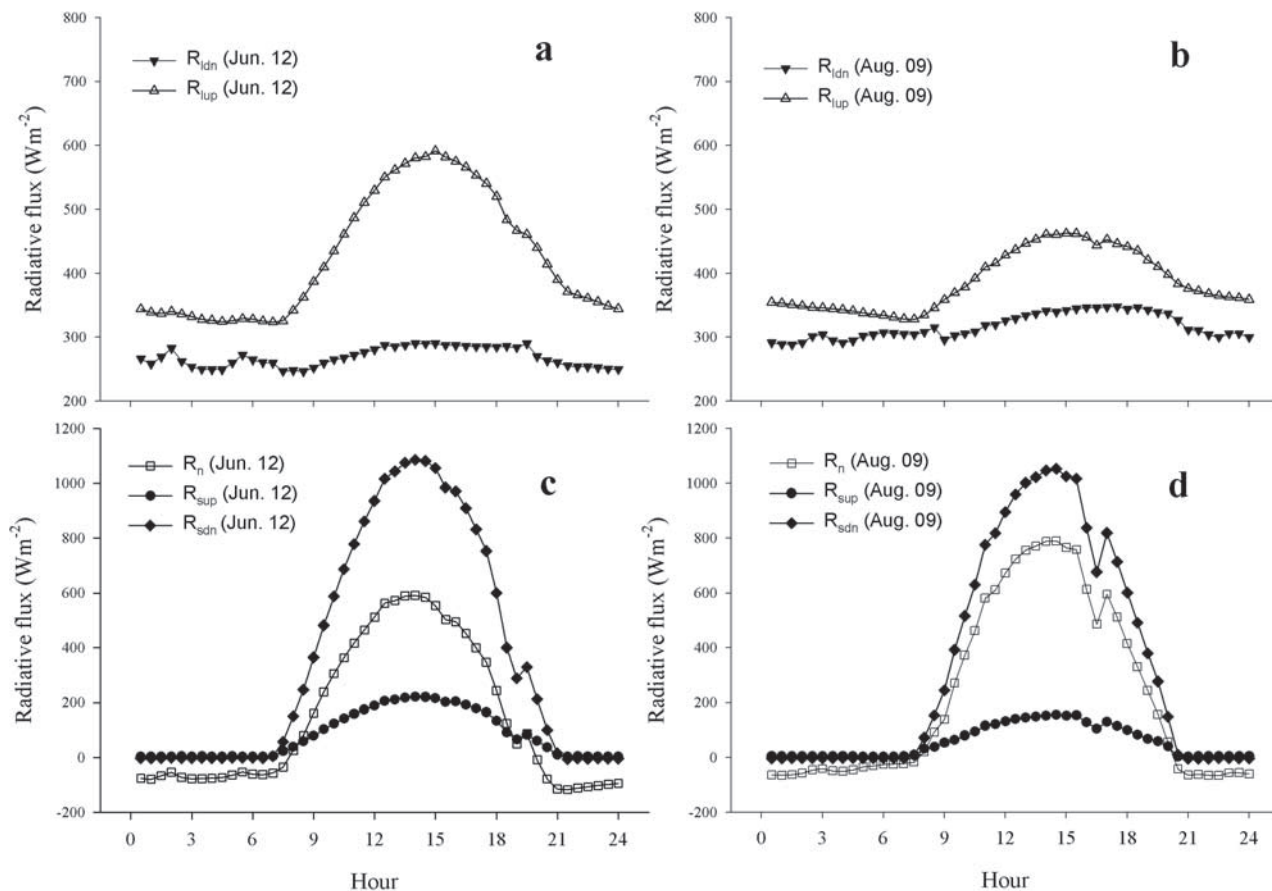


Figure 12. Diurnal variations of radiation budget components on 12 June (Figures 12a and 12c, premonsoon) and 9 August 1998 (Figures 12b and 12d, monsoon). R_{ldn} is the downward longwave radiation, R_{lup} is the outgoing longwave radiation, R_n is the net radiation, R_{sup} is the reflected shortwave radiation, and R_{sdn} is the incoming shortwave radiation.

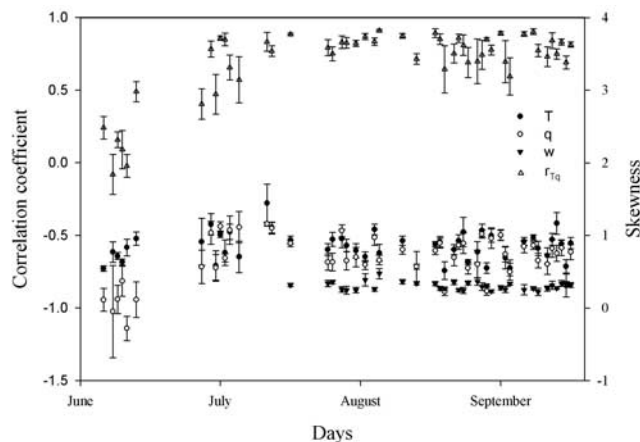


Figure 14. Seasonal variations of daytime-averaged r_{Tq} and skewness of T , q , and w . Error bars indicate standard error of mean.

pointed out by *De Bruin et al.* [1999], the relative contributions of entrainment of warm and dry air from the boundary layer top probably have influenced the similarity near the surface. Local advection or the heterogeneity of sink/source distributions of heat and water vapor also could result in dissimilarity between the two scalars [e.g., *Katul et al.*, 1995; *De Bruin et al.*, 1999]. Analysis of skewness under such influences would be helpful to better understand the turbulent exchange mechanisms over the Tibetan Plateau.

4. Concluding Remarks

[37] Turbulent exchange characteristics in a Tibetan shortgrass prairie were investigated in terms of flux variance relation, and the changes in environmental conditions, surface energy partitioning, and the similarity between heat and water vapor were presented with the seasonal march of the summer monsoon. Main results are summarized as follows.

[38] 1. Normalized standard deviations of heat and water vapor follow the Monin-Obukhov similarity theory. Heat and water vapor are similar in terms of the similarity constant, and the flux variance method produces comparable H and λE to those of eddy covariance method.

[39] 2. Unlike the similar magnitudes of transfer efficiency of heat and water vapor, momentum exchange is underestimated compared to the Monin-Obukhov similarity prediction.

[40] 3. As the summer monsoon progresses, significant changes in surface energy partitioning occur toward the enhancement of λE . The entrainment from boundary layer top or inversion layer aloft probably affects the dissimilarity between heat and water vapor during the premonsoon, whereas its effect during the monsoon seems relatively weak as evidenced by low β . More information is needed on the likely role of inactive eddies associated with turbulent exchange mechanisms over the plateau [*Hong et al.*, 2004].

[41] 4. Further direct measurements on turbulence statistics, evaluation of local advection and heterogeneity of source/sink distribution through remote sensing analysis,

and profile measurements of heat and water vapor in the boundary layer are needed, particularly for premonsoon periods. Such measurements are currently in progress on the plateau through ongoing CEOP field campaigns.

[42] **Acknowledgments.** We are grateful to Bert Tanner and Edward Swiatek at Campbell Scientific, Inc., for their prompt and generous lending of the sonic anemometer used in this study. Our thanks also go out to Y. Yupin for helping with field measurements. Financial support was given through the “Eco-Technopia 21 project” by the Ministry of Environment, Korea, and the National Space Development Agency of Japan. The CEOP data were provided within the framework of GAME/CAMP Tibet Scientific and Technological Research Project, funded by the Ministry of Education, Culture, Sports, Science and Technology; the Japan Science and Technology Agency; the Frontier Research System for Global Change; the Japan Aerospace Exploration Agency; the Chinese Academy of Sciences; and the Chinese Academy of Meteorological Sciences.

References

- Andreas, E. L., R. J. Hill, J. R. Gosz, D. I. Moore, W. D. Otto, and A. D. Sarma (1998), Statistics of surface-layer turbulence over terrain with metre-scale heterogeneity, *Boundary Layer Meteorol.*, **86**, 379–408.
- Asanuma, J., and W. Brutsaert (1999), Turbulence variance characteristics of temperature and humidity in the unstable atmospheric surface layer above a variable pine forest, *Water Resour. Res.*, **35**(2), 515–521.
- Bian, L., Z. Gao, Q. Xu, L. Lu, and Y. Cheng (2002), Measurements of turbulence transfer in the near-surface layer over the southeastern Tibetan Plateau, *Boundary Layer Meteorol.*, **102**, 281–300.
- Bink, N. J., and A. G. C. A. Meesters (1997), Comment on “Estimation of surface heat and momentum fluxes using the flux-variance method above uniform and non-uniform terrain” by Katul et al. (1995), *Boundary Layer Meteorol.*, **84**, 497–502.
- Chen, L., E. R. Reiter, and Z. Feng (1985), The atmosphere heat source over the Tibetan Plateau: May–August 1979, *Mon. Weather Rev.*, **113**, 1771–1790.
- De Bruin, H. A. R., W. Kohsiek, and B. J. J. M. Van Den Hurk (1993), A verification of some methods to determine the fluxes of momentum, sensible heat, and water vapor using standard deviation and structure parameter of scalar meteorological quantities, *Boundary Layer Meteorol.*, **63**, 231–257.
- De Bruin, H. A. R., B. J. J. M. Van Den Hurk, and L. J. M. Kroon (1999), On the temperature-humidity correlation and similarity, *Boundary Layer Meteorol.*, **93**, 453–468.
- Finnigan, J. J., R. Clements, Y. Malhi, R. Leuning, and H. A. Cleugh (2003), A re-evaluation of long-term flux measurement techniques. Part 1: Averaging and coordinate rotation, *Boundary Layer Meteorol.*, **107**, 1–48.
- Flohn, H. (1957), Large-scale aspects of the “summer monsoon” in south and east Asia, *J. Meteorol. Soc. Jpn.*, 75th anniv. vol., 180–186.
- Gao, Z., J. Wang, Y. Ma, J. Kim, T. Choi, H. Lee, J. Asanuma, and Z. Su (2000), Calculation of near-surface layer turbulent transport and analysis of surface thermal equilibrium features in Nagqu of Tibet, *Phys. Chem. Earth, Part B: Hydrol. Oceans Atmos.*, **25**, 135–139.
- Gao, Z., N. Chae, J. Kim, J. Hong, T. Choi, and H. Lee (2004), Modeling of surface energy partitioning, surface temperature and soil wetness in the Tibetan prairie using the Simple Biosphere Model 2 (SiB2), *J. Geophys. Res.*, **109**, D06102, doi:10.1029/2003JD004089.
- Högström, U. (2002), Theory and measurements for turbulence spectra and variances in the atmospheric neutral surface layer, *Boundary Layer Meteorol.*, **103**, 101–124.
- Hong, J., T. Choi, H. Ishikawa, and J. Kim (2004), Turbulence structures in the near-neutral surface layer on the Tibetan Plateau, *Geophys. Res. Lett.*, **31**, L15106, doi:10.1029/2004GL019935.
- Kaimal, J. C., and J. Finnigan (1994), *Atmospheric Boundary Layer Flows: Their Structure and Measurement*, Oxford Univ. Press, New York.
- Katul, G. G., and C.-I. Hsieh (1997), Reply to the comment by Bink and Meesters, *Boundary Layer Meteorol.*, **84**, 503–509.
- Katul, G. G., and C.-I. Hsieh (1999), A note on the flux-variance similarity relationships for heat and water vapor in the unstable atmospheric surface layer, *Boundary Layer Meteorol.*, **90**, 327–338.
- Katul, G. G., S. M. Goltz, C.-I. Hsieh, Y. Cheng, F. Mowry, and J. Sigmon (1995), Estimation of surface heat and momentum fluxes using the flux-variance method above uniform and non-uniform terrain, *Boundary Layer Meteorol.*, **74**, 237–260.
- Kim, J., et al. (2001), On measuring and modeling surface energy partitioning in a Tibetan prairie during GAME-IOP 1998, paper presented at the Fifth International Study Conference on GEWEX in Asia and GAME, World Clim. Res. Program, Nagoya, Japan, 3–5 Oct.

- Koike, T., T. Yasunari, J. Wang, and T. Yao (1999), GAME-Tibet IOP summary report, paper presented at the 1st International Workshop on GAME-Tibet, Chin. Acad. of Sci., Xian, China, 11–13 Jan.
- Li, C., and M. Yanai (1996), The onset and interannual variability of the Asian summer monsoon in relation to land-sea thermal contrast, *J. Clim.*, *9*, 358–375.
- Li, C., T. Duan, S. Haginoya, and L. Chen (2001), Estimates of the bulk transfer coefficients and surface fluxes over the Tibetan Plateau using AWS data, *J. Meteorol. Soc. Jpn.*, *79*(2), 625–635.
- Liu, X. D., J. E. Kutzbach, Z. Liu, Z. S. An, and L. Li (2003), The Tibetan Plateau as amplifier of orbital-scale variability of the east Asian monsoon, *Geophys. Res. Lett.*, *30*(16), 1839, doi:10.1029/2003GL017510.
- Luo, H., and M. Yanai (1983), The large-scale circulation and heat sources over the Tibetan Plateau and surrounding areas during the early summer of 1979: Part I. Precipitation and kinematic analyses, *Mon. Weather Rev.*, *111*, 922–944.
- Mahrt, L. (1991), Boundary-layer moisture regimes, *Q. J. R. Meteorol. Soc.*, *117*, 151–171.
- Mahrt, L. (1998), Flux sampling errors for aircraft and towers, *J. Atmos. Oceanic Technol.*, *15*, 416–429.
- McNaughton, K. G., and Y. Brunet (2002), Townsend's hypothesis, coherent structure and Monin-Obukhov similarity, *Boundary Layer Meteorol.*, *102*, 161–175.
- Moore, C. J. (1986), Frequency response corrections for eddy correlation systems, *Boundary Layer Meteorol.*, *37*, 17–35.
- Pahlow, M., M. B. Parlange, and F. Porté-Agel (2001), On Monin-Obukhov similarity in the stable atmospheric boundary layer, *Boundary Layer Meteorol.*, *99*, 225–248.
- Panofsky, H., and J. Dutton (1984), *Atmospheric Turbulence: Models and Methods for Engineering Application*, 397 pp., John Wiley, Hoboken, N. J.
- Pattey, E., I. B. Strachan, R. L. Desjardins, and J. Massheder (2002), Measuring nighttime CO₂ flux over terrestrial ecosystems using eddy covariance and nocturnal boundary layer methods, *Agric. For. Meteorol.*, *113*, 145–158.
- Smith, E. A., and L. Shi (1992), Surface forcing of the infrared cooling profile over the Tibetan Plateau. Part I: Influence of relative longwave radiative heating at high altitude, *J. Atmos. Sci.*, *49*, 805–822.
- Swinbank, W. C. (1951), The measurement of vertical transfer of heat, water vapor and momentum in the lower atmosphere with some results, *J. Meteorol.*, *8*, 135–145.
- Tillman, J. E. (1972), The indirect determination of stability, heat and momentum fluxes in the atmospheric boundary layer from simple scalar variables during dry unstable conditions, *J. Appl. Meteorol.*, *11*, 783–792.
- Van Den Hurk, B. J. J. M., and H. A. R. De Bruin (1995), Fluctuations of the horizontal wind under unstable conditions, *Boundary Layer Meteorol.*, *74*, 341–352.
- Weaver, H. (1990), Temperature and humidity flux-variance relations determined by one-dimensional eddy correlation, *Boundary Layer Meteorol.*, *53*, 77–91.
- Webb, E. K., G. I. Perman, and R. Leuning (1980), Correction of flux measurements for density effects due to heat and water transfer, *Q. J. R. Meteorol. Soc.*, *106*, 85–100.
- Wyngaard, J. C., O. R. Cote, and Y. Izumi (1971), Local free convection, similarity, and the budgets of shear stress and heat flux, *J. Atmos. Sci.*, *28*, 1171–1182.
- Yeh, D., and Y. X. Gao (1979), *The Meteorology of the Qinghai-Xizang (Tibet) Plateau*, 278 pp., Sci. Press, Beijing.
- Yeh, T.-C., S.-Y. Dao, and M.-T. Li (1957), The abrupt change of circulation over the North Hemisphere during June and October, in *The Atmosphere and the Sea in Motion, Rossy Memorial Volume*, pp. 249–267, Rockefeller Inst. Press, Albany, N. Y.
- J. Asanuma, Department of Geosciences, Tsukuba University, Tsukuba 305-8571, Japan. (asanuma@suiri.tsukuba.ac.jp)
- T. Choi, J. Hong, J. Kim, and H. Lee, Department of Atmospheric Sciences, Yonsei University, Seoul 120-749, Republic of Korea. (ctjin@yonsei.ac.kr; jkhong@yonsei.ac.kr; joon-kim@yonsei.ac.kr; fluxes@atmos.yonsei.ac.kr)
- Gao Zhiqiu, Chinese Administration for Meteorological Sciences, Beijing 100081, China. (zgao@cams.cma.gov.cn)
- H. Ishikawa, Disaster Prevention Research Institute, Kyoto University, Kyoto 611-0011, Japan. (ishikawa@storm.dpri.kyoto-u.ac.jp)
- T. Koike, Department of Civil Engineering, University of Tokyo, Tokyo 113-8656, Japan. (tkoike@hydra.t.u-tokyo.ac.jp)
- Y. Ma and K. Ueno, School of Environment, University of Shiga Prefecture, Hassaka-cho 2500, Hikone, Shiga 522-8533, Japan. (ymma@ns.lzb.ac.cn; kueno@ses.ups.ac.jp)
- O. Tsukamoto, Faculty of Science, Okayama University, 3-1-1 Tsushima-naka, Okayama 700-8530, Japan. (tsuka@cc.okayama-u.ac.jp)
- J. Wang, Cold and Arid Regions Environmental and Engineering Research Institute, Chinese Academy of Sciences, Lanzhou 730000, China. (jmwang@ns.lzb.ac.cn)
- T. Yasunari, Hydrospheric Atmospheric Research Center, Nagoya University, Nagoya 464-8601, Japan. (yasunari@hyarc.nagoya-u.ac.jp)